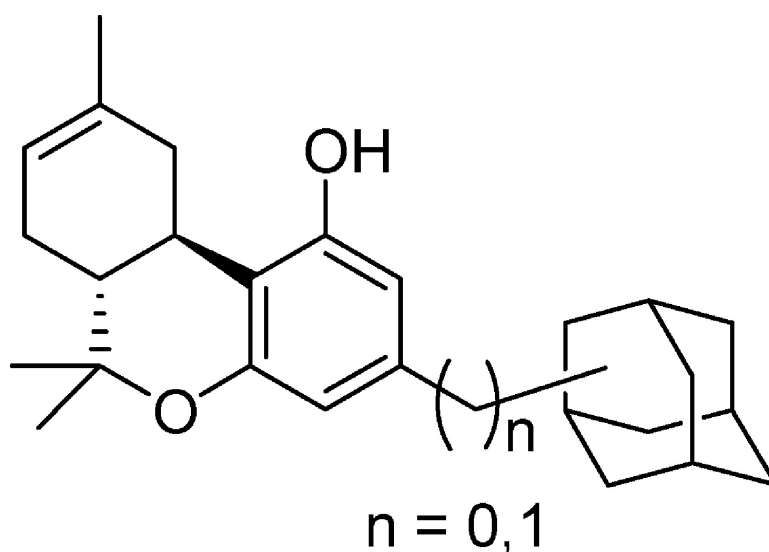


Adamantyl Cannabinoids: A Novel Class of Cannabinergic Ligands

Dai Lu, Zhaoxing Meng, Ganesh A. Thakur, Pusheng Fan, John Steed, Cindy L. Tartal, Dow P. Hurst, Patricia H. Reggio, Jeffrey R. Deschamps, Damon A. Parrish, Clifford George, Torbjørn U. C. Jrbe, Richard J. Lamb, and Alexandros Makriyannis

J. Med. Chem., **2005**, 48 (14), 4576-4585 • DOI: 10.1021/jm058175c • Publication Date (Web): 16 June 2005

Downloaded from <http://pubs.acs.org> on March 28, 2009



More About This Article

Additional resources and features associated with this article are available within the HTML version:

- Supporting Information
- Links to the 7 articles that cite this article, as of the time of this article download
- Access to high resolution figures
- Links to articles and content related to this article
- Copyright permission to reproduce figures and/or text from this article

[View the Full Text HTML](#)

Adamantyl Cannabinoids: A Novel Class of Cannabinergic Ligands

Dai Lu,[†] Zhaoxing Meng,[†] Ganesh A. Thakur,[†] Pusheng Fan,[†] John Steed,[‡] Cindy L. Tartal,[‡] Dow P. Hurst,[‡] Patricia H. Reggio,[‡] Jeffrey R. Deschamps,^{||} Damon A. Parrish,^{||} Clifford George,^{||} Torbjörn U. C. Järbe,[§] Richard J. Lamb,[⊥] and Alexandros Makriyannis^{*,†}

Center for Drug Discovery, Northeastern University, 360 Huntington Avenue, 116 Mugar Life Sciences Building, Boston, Massachusetts 02115, Department of Chemistry and Biochemistry, University of North Carolina—Greensboro, Greensboro, North Carolina 27402, Naval Research Laboratory, Code 6030, Washington, D.C. 20375, Department of Psychology, Temple University, Philadelphia, Pennsylvania 19122, and Departments of Psychiatry and Pharmacology, University of Texas Health Science Center at San Antonio, San Antonio, Texas 78229

Received January 21, 2005

Structure–activity relationship studies have established that the aliphatic side chain plays a pivotal role in determining the cannabinergic potency of tricyclic classical cannabinoids. We have now synthesized a series of analogues in which a variety of adamantyl substituents were introduced at the C3 position of Δ^8 -THC. Our lead compound, (–)-3-(1-adamantyl)- Δ^8 -tetrahydrocannabinol (**1a**, AM411), was found to have robust affinity and selectivity for the CB1 receptor as well as high in vivo potency. The X-ray crystal structure of **1a** was determined. Exploration of the side chain conformational space using molecular modeling approaches has allowed us to develop cannabinoid side chain pharmacophore models for the CB1 and CB2 receptors. Our results suggest that although a bulky group at the C3 position of classical cannabinoids could be tolerated by both CB1 and CB2 binding sites, the relative orientation of that group with respect to the tricyclic component can lead to receptor subtype selectivity.

Introduction

Δ^9 -Tetrahydrocannabinol (Δ^9 -THC), the active ingredient of marijuana (*Cannabis sativa*),¹ binds almost equally to the two known G-protein-coupled cannabinoid receptors CB1^{2,3} and CB2.⁴ CB1 is found in the central nervous system (CNS), as well as in a number of organs in the periphery, while CB2 is principally associated with the immune system.⁵ The search for cannabinoids possessing a high degree of pharmacological potency and selectivity has led to the synthesis and testing of a large number of novel analogues^{6–9} from which structure–activity relationships (SAR) could be established. Four pharmacophores associated with cannabimimetic activity¹⁰ were recognized within the classical and nonclassical cannabinoid prototypes. These include a phenolic hydroxyl, a lipophilic alkyl side chain, a northern aliphatic hydroxyl group also found in the metabolites of the plant-derived cannabinoids, and a southern aliphatic hydroxyl first introduced in the nonclassical class of cannabinoids developed by Pfizer and represented by the well-known ligand CP-55,940, (–)-3-[2-hydroxy-4-(1,1-dimethylheptyl)phenyl]-4-(3-hydroxypropyl)cyclohexan-1-ol.

The significance of the aliphatic side chain was first demonstrated by Adams, who showed that substitution of the *n*-pentyl side chain of Δ^9 -THC with a 1',1'-dimethylheptyl group led to a 100-fold increase in potency.^{11,12} Subsequent work has established that the side chain plays a pivotal role in modulating cannab-

inergic potency.^{13–19} Earlier work from our laboratory has explored the pharmacophoric requirements of the side chain within the classical tetrahydrocannabinol (THC) template. This included conformational restriction through the inclusion of multiple bonds within the chain, the addition of C1' cyclic substituents,^{17,18} and the incorporation of the first one or two side chain carbons into a six-membered ring fused with the phenolic A ring.¹⁹ This led to a series of cannabinergic ligands possessing enhanced affinity and selectivity for both CB1 and CB2 receptors.

To add to our present understanding of the possible conformation of the side chain adopted during interaction with the active site, we have developed novel analogues carrying bulky and/or rigid aliphatic substituents at the 3-position of the phenolic A ring. Here we describe the synthesis of a carefully designed series of analogues, in which a variety of adamantyl substituents were introduced at the C3 position of the phenolic ring of Δ^8 -THC (Figure 1). Exploration of the allowable conformational space for these side chains provided us with insights regarding the pharmacophoric features required for CB1 and CB2 selectivities. We also used computational modeling studies to outline steric differences between the different side chain substitutions that define receptor subtype recognition. Our results shed new light on the bioactive conformation of the classical cannabinoid side chain as well as the side chain subsites within the CB1 and CB2 receptors. Our lead compound **1a** (AM411), the first pharmacologically active^{20,21} classical cannabinoid to be crystallized, was found to possess substantial CB1 selectivity and high in vivo potency.

Chemistry. Generally, the synthesis of adamantyl congeners of Δ^8 -THC (**1a–e**) was achieved by condensation of the chiral monoterpene alcohol (+)-*cis/trans*-*p*-mentha-2,8-dien-1-ol with an appropriately 5-substi-

* Corresponding author. Phone: 617-373-4200; Fax: 617-373-7493; E-mail: a.makriyannis@neu.edu.

[†] Northeastern University.

[‡] University of North Carolina—Greensboro.

^{||} Naval Research Laboratory.

[§] Temple University.

[⊥] University of Texas Health Science Center at San Antonio.

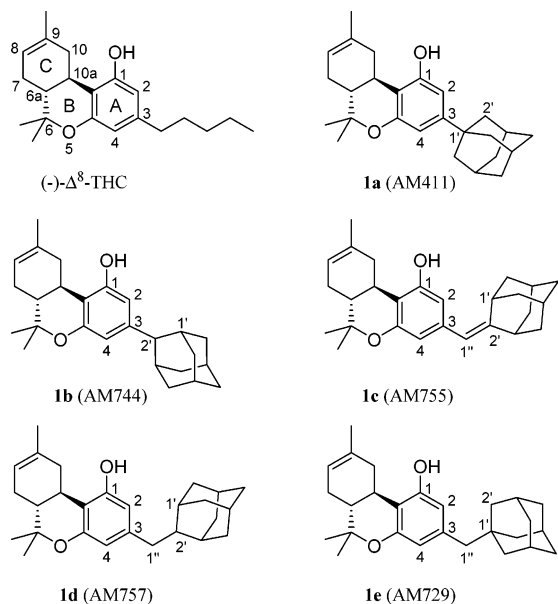
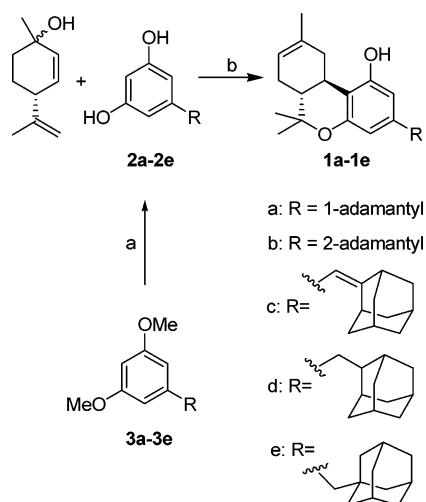


Figure 1. (-)- Δ^8 -THC and target compounds (**1a–e**) used to examine the effects of steric bulk and rigidity at the side chain of classical cannabinoids.

Scheme 1^a



^a Reagents and conditions: (a) BBr_3 , CH_2Cl_2 , 0 °C to rt; (b) p -TSA, CHCl_3 , 65 °C, 6 h.

tuted resorcinol. Following a well-established protocol,^{19,22,23} condensation (Scheme 1) of resorcinol derivatives **2a–e** with (+)-*cis/trans*-*p*-mentha-2,8-dien-1-ol catalyzed by *p*-toluenesulfonic acid monohydrate afforded the corresponding tetrahydrocannabinol analogues **1a–e** (Table 1) in 40–84% yield.

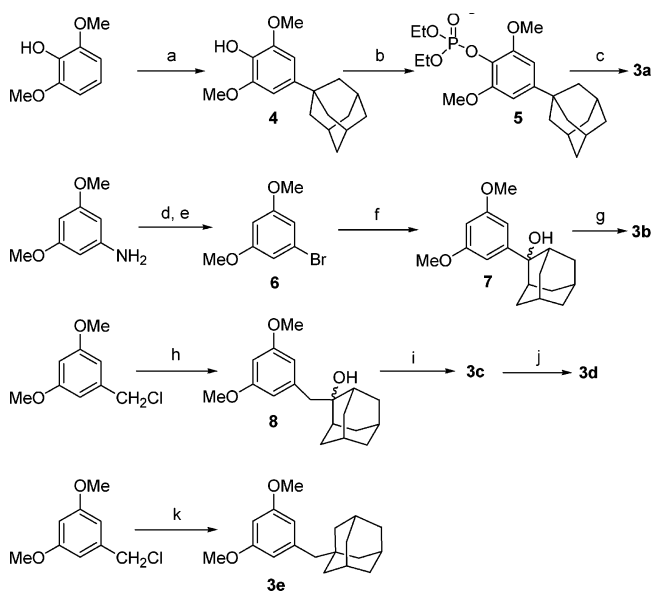
The dimethylated resorcinol **3a** was synthesized by following a previously reported procedure.²⁴ Alkylation of 2,6-dimethoxyphenol with 1-adamantanol in the presence of methanesulfonic acid gave **4** as the predominant isomer (Scheme 2). This was converted to the phosphate ester **5** using diethylphosphonate in a 75% yield, and then treatment of **5** with Li/NH_3 at -78 °C gave the 5-alkylresorcinol dimethyl ether **3a** in a 70% yield. The 5-alkylresorcinol dimethyl ether **3b** was prepared from commercially available 3,5-dimethoxyaniline. Diazotization of 3,5-dimethoxyaniline followed by its exposure to cuprous bromide gave 1-bromo-3,5-dimethoxybenzene (**6**) in 56% yield. Addition of 2-adamantanone to the organomagnesium reagent derived

Table 1. Affinities (K_i) of Δ^8 -THC Analogues for CB1 and CB2 Cannabinoid Receptors^a

Compound	R	CB1 (K_i , nM) ^a	CB2 (K_i , nM) ^a
1a		6.80 (6.0–7.3)	52.0 (47.0–60.8)
1b		34.9 (29.0–42.1)	14.0 (11.7–16.9)
1c		48.6 (44.8–52.8)	8.9 (8.2–9.6)
1d		79.7 (68.3–85.1)	76.0 (63.8–80.5)
1e		29.3 (26.4–35.6)	26.9 (22.7–31.4)
(-)- Δ^8 -THC	$n\text{-C}_5\text{H}_{11}$	47.6 (40.2–56.2)	39.3 (35.2–46.2)

^a Affinities for CB1 and CB2 were determined using rat brain (CB1) or mouse spleen (CB2) membranes and [^3H]CP-55,940 as the radioligand following previously described procedures.²⁷ K_i values were obtained from three independent experiments run in duplicate and are expressed as the mean of the three values, 95% confidence limits are indicated in parentheses.

Scheme 2^a



^a Reagents and conditions: (a) 1-adamantanol, $\text{CH}_3\text{SO}_3\text{H}$, 80 °C to rt; (b) $\text{H}(\text{O})\text{P}(\text{OEt})_2$, Et_3N , CCl_4 , 0 °C to rt; (c) Li/NH_3 , $\text{Et}_2\text{O}/\text{THF}$, -78 °C; (d) NaNO_2 , HBr ; (e) CuBr , HBr ; (f) Mg , THF , 2-adamantanone; (g) Li/NH_3 , THF , -60 °C; (h) Mg , Et_2O , 2-adamantanone; (i) p -TSA, CH_2Cl_2 , reflux; (j) $\text{H}_2/\text{Pd}-\text{C}$, EtOH , rt; (k) Mg , Et_2O , 1-bromo-2-adamantanone, heating.

from **6** gave carbinol **7** (68% yield), which when further treated with lithium in liquid ammonia gave **3b** in 78% yield. The remaining three 5-alkylresorcinol dimethyl ethers **3c**, **3d**, and **3e** were synthesized from commercially available 3,5-dimethoxybenzyl chloride. The

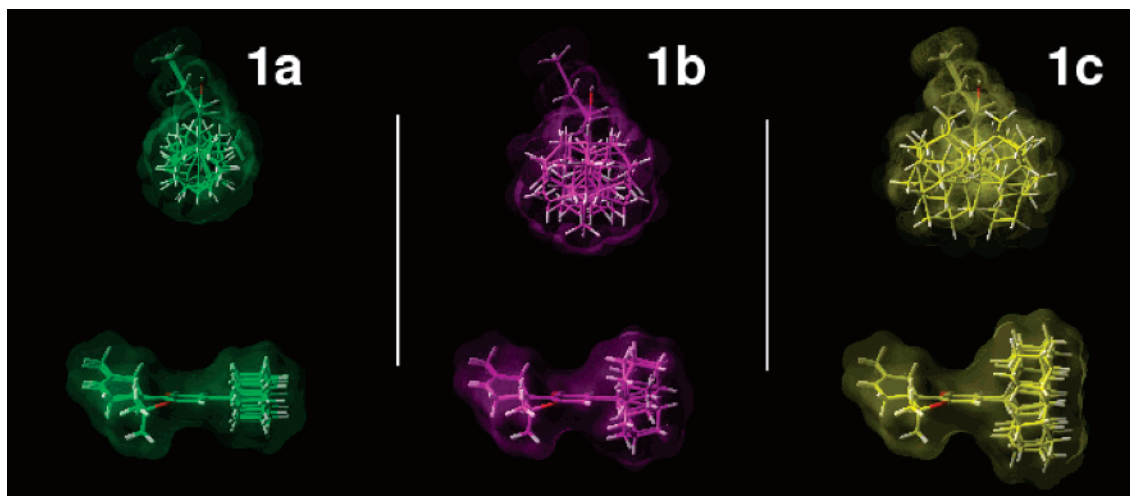


Figure 2. AM1 conformational search results for compounds **1a–c** are illustrated here. All accessible conformers for each ligand are shown superimposed at their aromatic rings and contoured at their van der Waals radii. (Top Row) For each conformer superposition in this view, the aromatic ring has been turned perpendicular to the plane of the page with the adamantyl substituent closest to the viewer and the carbocyclic ring furthest from the viewer. (Bottom Row) A bottom view of each conformer superposition for compounds **1a–c** is shown here. In this view, the aromatic ring of each conformer is oriented perpendicular to the plane of the page, with the long axis of each molecule horizontal. C4 is closest to the viewer and the phenolic hydroxyl is furthest from the viewer.

corresponding Grignard reacted with 2-adamantanone to give carbinol **8** in 80% yield. This was further dehydrated to **3c** in 83% yield under acidic conditions and catalytically reduced to provide the 5-alkylresorcinol dimethyl ether **3d** in nearly quantitative yield. Intermediate **3e** was obtained through a Wurtz-like coupling reaction^{25,26} between 1-bromoadamantane and the Grignard reagent derived from 3,5-dimethoxybenzyl chloride. Generally, the above reaction produced relatively low yields of product with the best result (24% yield) being obtained when high concentrations of reactants were used. Resorcinols **2a–e** were obtained from **3a–e**, respectively, by demethylation (85–95% yields).

Results and Discussion

Receptor Binding Studies. The compounds reported in this study are Δ^8 -THC analogues in which the C3 five carbon side chain of Δ^8 -THC was replaced with bulky adamantyl substituents. As with earlier work, we used (–)- Δ^8 -THC as our prototype, favoring it over the less stable and almost equipotent isomer (–)- Δ^9 -THC. The abilities of **1a–e** to displace radiolabeled CP-55,940 from purified rat forebrain synaptosomes²⁷ and mouse spleen membranes²⁸ were determined. Inhibition constant values (K_i)²⁹ calculated from the respective displacement curves are listed in Table 1 and serve as indicators for the affinities of these Δ^8 -THC analogues for the CB1 and CB2 receptors. As can be seen in Table 1, the range of K_i values of the five analogues indicates that structural modifications of the C3 adamantyl substituents on the Δ^8 -THC template can have profound effects on CB1/CB2 affinities and selectivities. Interestingly, replacing the linear side chain of Δ^8 -THC with bulky adamantyl groups did not abolish binding affinity. The 3-(1-adamantyl)- Δ^8 -THC analogue **1a** exhibited robust affinity (6.8 nM) for CB1 exceeding that of Δ^8 -THC and has significant CB1/CB2 selectivity. Conversely, the 3-(2-adamantyl)- Δ^8 -THC analogue **1b** is more CB2-selective. When the 1-adamantyl group of **1a**

is positioned further from the aromatic A ring by the introduction of a methylene link **1e**, affinity for CB1 receptor is reduced and there is no CB1/CB2 selectivity. Similarly, introduction of a methylene link in the 2-adamantyl position **1d** further reduced affinity and again eliminated CB1/CB2 selectivity. The compound with the highest CB2 selectivity was one in which the adamantyl group was linked at its 2-position to the aromatic ring through a styrene double bond. This compound **1c** also exhibited improved CB2 affinity (8.9 nM).

Examination of the CB1 and CB2 affinities for the five analogues included in this study indicated that both receptor subtypes are capable of accommodating bulky groups in the 3-position of the tricyclic cannabinoid structure. However, compounds **1a–e** also exhibited differences in their relative affinities for the two receptor subtypes. We postulated that these observed differences in the relative ability of each ligand to interact with the CB1 and CB2 sites could be accounted for by examining their respective allowable conformational spaces. Therefore, we first used computer modeling to calculate the accessible conformers of compounds **1a–e**. Then the van der Waals volume maps and the Unique Volume Maps for the CB1 selective **1a**, the CB2 selective **1c**, and the nonselective **1d** were analyzed.

Computational Study. Conformational Analysis Results. Spartan conformational analysis identified four accessible conformers for **1a**, six accessible conformers for **1b**, **1c**, and **1d** and two accessible conformers for **1e** (see Supporting Information for further details). Figures 2 and 3 illustrate the conformational analysis results with accessible conformers superimposed at their benzene rings. Two graphical representations for each of the resultant superimposed structures have been illustrated. In the first (shown at the top of Figures 2 and 3), the fused ring structure is vertical and is oriented perpendicular to the plane of the page with the adamantyl group closest to the viewer and the carbocyclic C ring furthest from the viewer. In this

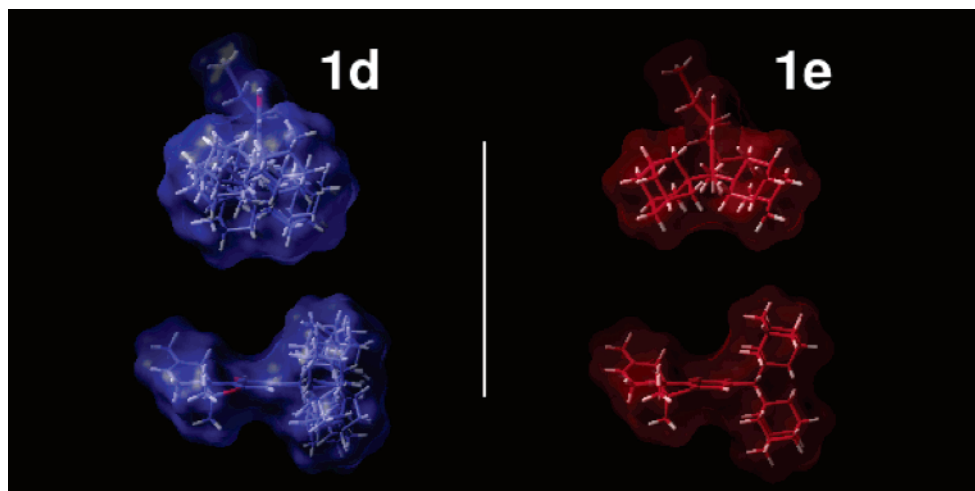


Figure 3. AM1 conformational search results for compounds **1d,e** are illustrated here. All accessible conformers for each ligand are shown superimposed at their aromatic rings and contoured at their van der Waals radii. (Top Row) For each conformer superposition in this view, the aromatic ring has been turned perpendicular to the plane of the page with the adamantyl substituent closest to the viewer and the carbocyclic ring furthest from the viewer. (Bottom Row) A bottom view of each conformer superposition for compounds **1d,e** is shown here. In this view, the aromatic ring of each conformer is oriented perpendicular to the plane of the page, with the long axis of each molecule horizontal. C4 is closest to the viewer and the phenolic hydroxyl is furthest from the viewer.

orientation the top face of the molecule is to the left of the fused ring system and the bottom face is to the right of the fused ring system. In the second representation (shown at the bottom of Figures 2 and 3), the fused ring structure is oriented along the horizontal direction and perpendicular to the plane of the page such that the C1 phenolic hydroxyl is furthest from the viewer and C4 is closest (see numbering system for Δ^8 -THC in Figure 1). In this orientation, the top face of the molecule is above the plane of the fused ring structure and the bottom face is below the plane.

Experimental results reported in Table 1 indicate that the change in the attachment point for C3 to the adamantyl group from compound **1a** to **1b** resulted in a shift from CB1 to CB2 selectivity. It is clear from Figure 2 (**1a** and **1b**) that the site of attachment for C3 to the adamantyl group has a significant effect on the volume of space that the adamantyl group can occupy. Attachment of C3 to a bridgehead position (C1') on the adamantyl group as in **1a** resulted in the adamantyl group orienting symmetrically such that the plane of the aromatic A ring bisects the adamantyl group. Attachment of C3 to a nonbridgehead atom (C2') as in **1b** resulted in the adamantyl group being able to occupy more space clearly extending into the top and bottom faces of the ligand.

It is clear from Figures 2 and 3 that the introduction of a methylene spacer (C1'') between C3 and the adamantyl group in compounds **1c**, **1d**, and **1e** also led to the adamantyl group being able to occupy more volume in the top and bottom faces of the molecules. In compounds **1c** and **1d**, attachment of the adamantyl group to the methylene spacer and C3 was via the nonbridgehead C2' position. Although rotation about the C3–C1'' bond was possible for both **1c** and **1d**, rotation about the C1''–C2' bond was restricted for compound **1c** due to the presence of the C1''–C2' double bond. As is indicated in Table 1, this structural variation had a profound effect on affinity, as **1c** showed the highest CB2 selectivity in the series and **1d** exhibited the poorest affinity (both for CB1 and CB2) in the series.

Compound **1e** was the only compound for which several conformers were above the 2.00 kcal/mol cutoff for accessibility in this study. Conformers that placed the adamantyl group in the plane of the fused ring system (C2–C3–C1''–C1' = -179.8° and 0.8°) were highest in energy (3.48 and 3.63 kcal/mol, respectively).

Table 1 indicates that in the progression from **1a** to **1b** to **1c**, CB2 selectivity increases. Modeling studies indicate that the major change in going from **1a** to **1b** to **1c** is an ability to place the adamantyl group further into the top and bottom faces of the molecules. This is illustrated in Figure 2 by the wider arc in the form of a donut transcribed by the adamantyl group in the allowed conformers of each compound as one moves from **1a** to **1b** to **1c**. On the other hand, the CB1 selectivity of **1a** can be associated with the conformationally allowable space of the 1-adamantyl group represented by the smaller symmetrical sphere attached to the C3 carbon of the tricyclic cannabinoid structure.

Unique Volume Map Calculations. When interpreted together with receptor binding data, our conformational analysis results suggested that there is a difference in the requirements for a C3 adamantyl group interaction with the respective hydrophobic pockets within CB1 or CB2. To illustrate the key conformational differences between the CB1 selective 3-(1-adamantyl)-THC **1a** and the CB2 selective 3-(2-adamantylidene)-methyl-THC **1c**, we used a modification of the Active Analog Approach³⁰ to calculate the volume of space that is unique to the CB2 selective analogue **1c** using all accessible conformers of **1a** and **1c** identified by AM1 Conformational Search calculations. In Figure 4a, the global minimum energy conformer of **1a** is shown in green tube display and in the same orientation as shown in the top row of Figure 2. The purple grid shows the union of the van der Waals volume maps of all accessible conformers of **1a** superimposed at their aromatic rings. The global minimum energy conformer of compound **1c** is illustrated in green tube display in Figures 4b and 4c. The yellow grid area in Figure 4b represents that region of the van der Waals space of all conformers of

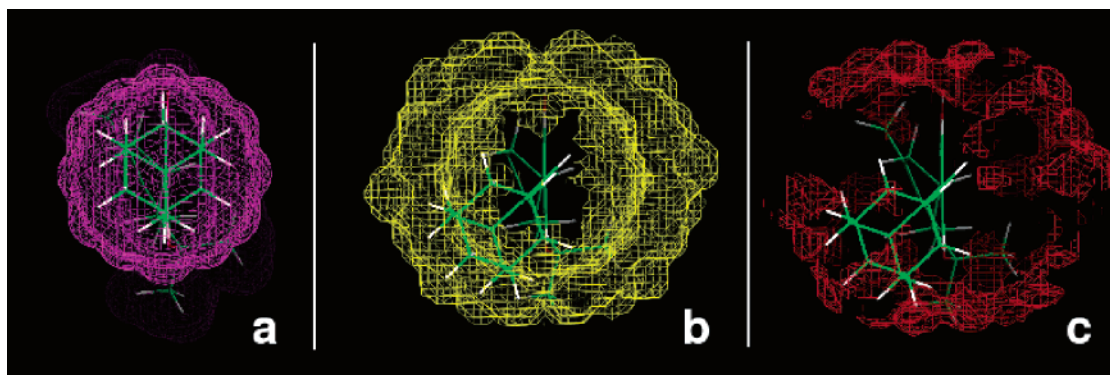


Figure 4. In each of the volume map calculations illustrated here, the view is such that the aromatic ring of subject molecules has been turned perpendicular to the plane of the page with the adamantyl substituent closest to the viewer and the carbocyclic ring furthest from the viewer. (a) This figure illustrates the union of the van der Waals volume of all accessible conformers of the CB1 selective compound **1a** (purple grid). The global minimum energy conformer of **1a** is shown in green tube display here. (b) This figure illustrates the Unique Volume Map calculated using all conformers of the CB1 selective compound **1a** and of the CB2 selective compound **1c**. The global minimum energy conformer of compound **1c** is shown here in green tube display. The yellow grid area shows the region of space into which conformers of **1c** protrude that is not shared with the accessible conformers of **1a**. (c) This figure illustrates the Unique Volume Map calculated using all conformers of the CB2 selective compound **1c** and of the nonselective compound **1d**. The global minimum energy conformer of **1c** is shown here in green tube display. The red grid area shows the region of space into which conformers of **1c** protrude that is not shared with the accessible conformers of **1d**.

1c that is *not* occupied by the conformers of **1a**. This Unique Volume Map provides an illustration of the extent to which the adamantyl group can be placed away from the plane of the aromatic ring in the most CB2 selective analogue **1c**. This map can be interpreted as encompassing that region of space occupied by adamantyl-THC analogues in order to selectively interact with the CB2 receptor.

In compounds **1c** and **1d**, a methylene spacer is located between C3 and the adamantyl group, and the attachment of the adamantyl group to the methylene spacer is via a nonbridgehead (C2') position. Although rotation about the C3–C1'' bond is possible for both **1c** and **1d**, rotation about the C1''–C2' bond in **1c** is restricted by the C1''–C2' double bond. The Unique Volume Map illustrated in Figure 4c shows that region of space (red grid) that is unique to the CB2 selective compound **1c** when compared to the nonselective compound **1d**. This map can also be interpreted to indicate unique regions in both the top and bottom faces of the molecule associated with favorable interaction with the CB2 subsite for the side chain of this class of compounds.

Crystal Structure of 3-(1-Adamantanyl)-6,6,9-trimethyl-6a,7,10,10a-tetrahydro-6H-benzo[*c*]-chromen-1-ol (1a**).** The three-dimensional structure of **1a** (Figure 5) was determined by X-ray crystallography, which showed a great deal of correspondence with the computationally determined one. Detail of the structural data is shown in the Experimental Section and with the Supporting Information.

In the crystal structure, the pyran and the cyclohexene rings exist in half-chair conformations, of which the O(5)–C(4A)–C(10B)–C(10A)–C(6A) atoms are in a slightly twisted plane, and C(6) is away from the plane by about 24° (Figure 5, Table 2). The phenolic ring also has a slight twist, with the adamantyl group bisecting the aromatic ring.

Prior to the determination of the crystal structure of **1a**, the crystal structures of naturally occurring cannabidiol³¹ and Δ^9 -tetrahydrocannabinolic acid b³² were reported. However, those two molecules have only weak

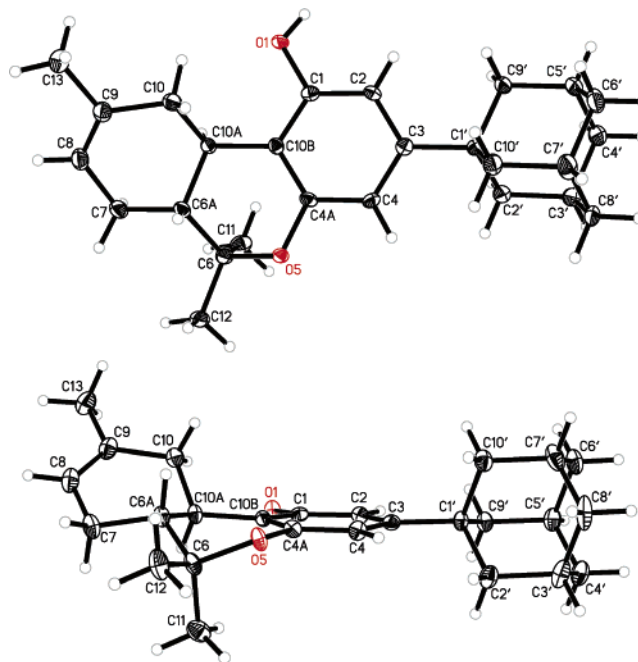


Figure 5. Thermal ellipsoid plot of **1a** is shown with the aromatic C ring facing the viewer (top) and with the aromatic C ring perpendicular to the paper (bottom). Ellipsoids are at the 30% probability level. Oxygen is shown in red color.

affinities for CB1 and CB2 and cannot be considered suitable models for the pharmacophoric requirements at the CB1/CB2 sites. Conversely, compound **1a** exhibits high affinity for the CB1 receptor and high *in vivo* potency. Therefore, the crystal structure of **1a** may provide the best available model for understanding ligand interactions with the CB1 cannabinoid receptor.

In Vivo Cannabinergic Activity. We have tested the *in vivo* cannabinergic properties of **1a** in rats using a drug discrimination assay as described earlier.³³ Compound **1a** was evaluated at three time intervals after administration (30, 90, and 270 min post) in doses ranging from 0.03 to 1.8 mg/kg. The ED₅₀ values are listed in Table 3. The outcome of the *in vivo* assay suggested that **1a** is a full agonist that is more potent

Table 2. Some Torsion Angles [deg] for Crystalline **1a**

atom and bond connection ^a	torsion angles [deg]
O(5)–C(4A)–C(10B)–C(10A)	3.1(2)
O(5)–C(4A)–C(10B)–C(1)	–175.61(13)
C(4A)–C(10B)–C(10A)–C(6A)	4.8(2)
C(1)–C(10B)–C(10A)–C(6A)	–176.52(14)
C(4)–C(4A)–C(10B)–C(10A)	–177.14 (15)
C(10B)–C(4A)–O(5)–C(6)	24.2(2)
C(4)–C(4A)–O(5)–C(6)	–155.58(13)
C(7)–C(8)–C(9)–C(10)	6.4(3)
C(8)–C(9)–C(10)–C(10A)	10.1(2)
C(10B)–C(10A)–C(10)–C(9)	–168.92(13)
C(6A)–C(10A)–C(10)–C(9)	–45.85(17)
C(4A)–C(10B)–C(10A)–C(6A)	4.8(2)
C(4A)–C(10B)–C(10A)–C(10)	126.48(16)

^a The atom numbering system is illustrated in Figure 5. Complete data of torsion angles are available in Supporting Information.

Table 3. Drug Discrimination Test with **1a**^a

drug	time (h)	ED ₅₀ (mg/kg)
Δ^9 -THC	0.5	1.16 (0.73–1.58)
1a	0.5	0.68 (0.47–0.90)
1a	1.5	0.44 (0.06–0.82)
1a	4.5	0.41 (0.09–0.72)

^a ED₅₀ values (\pm 95% C.L.) for **1a** and Δ^9 -THC for animals trained to discriminate between 3 mg/kg Δ^9 -THC and vehicle, injected ip 30 min prior to training session onset. The doses examined were: **1a** (0.03, 0.1, 0.3, 0.56, 1, and 1.8 mg/kg); Δ^9 -THC (0.1, 0.3, 1, 1.8, and 3 mg/kg).

than Δ^9 -THC in this assay, with perhaps a slower onset time and a longer duration of action as compared to Δ^9 -THC.^{34,35} Figure 6 shows that the CB1-selective

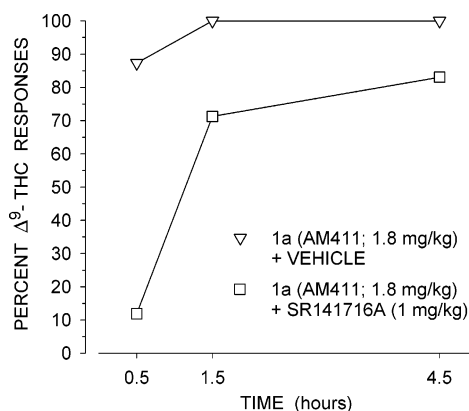


Figure 6. Generalization test results for **1a** alone and in combination with SR141716A at three postinjection intervals for rats trained to discriminate between 3 mg/kg Δ^9 -THC and vehicle ($n = 8$). The generalization test results represent the mean percentage of lever presses on the Δ^9 -THC appropriate lever out of the total number of lever presses emitted during a six trial test probe (Y-axis); time in hours since injection (X-axis).

antagonist SR141716A³⁶ (1 mg/kg) antagonized the discriminative stimulus effects of 1.8 mg/kg **1a** 30 min postinjection. The antagonism was reduced at 1.5 and 4.5 h post administration. A two-way repeated ANOVA indicated no significant Dose \times Time interaction [$F = 6.88$ (2, 14); $p = 0.052$] with regard to the rate of responding (responses/second) associated with the tests evaluating antagonism of **1a** by SR141716A.

Summary

Our study focused on introducing bulky adamantyl substituents in the 3-position of the classical cannab-

inoid Δ^9 -THC in lieu of the native *n*-pentyl chain. Testing of the five ligands included in this study for their affinities for the CB1 and CB2 receptors revealed that the bulky adamantyl group can easily be accommodated within the CB1 and CB2 binding sites. The results also revealed that variations in the adamantyl substituents can lead to higher affinities and selectivities for each of the two receptors depending on the relative orientation of the adamantyl group with respect to the tricyclic cannabinoid structure. Computational modeling suggested that the differences in affinities and selectivities can be explained on the basis of the allowable conformational space of each substituent.

The 3-(1-adamantyl) group of the CB1 selective analogue **1a** orients within a compact spherical space in the direct proximity of the tricyclic ring. Conversely, in the CB2 selective analogues **1b** and **1c**, the allowable adamantyl group conformations exist within a donut like space that extends beyond that of the spherical conformational space of **1a**. Finally, ligands capable of occupying both spaces (**1d**, **1e**) exhibit no CB1/CB2 selectivity. The crystal structure of our lead compound **1a** was compatible with the computationally determined 3D-structure. Compound **1a** was shown to be a long acting CB1 receptor agonist. Coupled with its favorable physical properties, the compound's potency and selectivity support its potential as a useful pharmacological lead.

Experimental Section

Chemistry. (+)-*cis/trans*-*p*-Mentha-2,8-dien-1-ol was supplied by Firmenich Inc., Princeton, NJ. All other reagents and solvents were purchased from Aldrich, Milwaukee, WI, unless specified otherwise and were used without further purification. All anhydrous reactions were performed under a static argon or nitrogen atmosphere in flame-dried glassware using scrupulously dry solvents. Organic phases were dried over Na₂SO₄ and rotary evaporated under reduced pressure, and flash column chromatography employed silica gel 60 (230–400 mesh, Selecto Scientific Inc., Suwanee, GA). All compounds were demonstrated to be homogeneous by analytical thin-layer chromatography (TLC) on precoated silica gel TLC aluminum plates (Whatman, UV₂₅₄, layer thickness 250 μ m), and chromatograms were visualized under ultraviolet light or by phosphomolybdic acid straining. Melting points were determined on a capillary Electrothermal melting point apparatus and are uncorrected. ¹H NMR spectra were recorded on a Bruker DMX-500 spectrometer operating at 500 MHz. All NMR spectra were recorded using CDCl₃ as solvent unless otherwise stated and chemical shifts are reported in ppm (parts per million) relative to tetramethylsilane as internal standard. Multiplicities are indicated as br (broadened), s (singlet), d (doublet), t (triplet), q (quartet), m (multiplet), bs (broadened singlet), and coupling constants (J) are reported in hertz (Hz). Low- and high-resolution mass spectra were performed at the School of Chemical Sciences, University of Illinois at Urbana-Champaign, or were recorded on a Hewlett-Packard 6890 GC/MS instrument at the School of Pharmacy, University of Connecticut. Elemental analyses were obtained at Baron Consulting Co., Milford, CT.

General Procedure A: Preparation of 5-Alkylresorcinols (2a–e) from 5-Alkyl-1,3-dimethoxybenzenes (3a–e). 4.1 mL of 1.0 M boron tribromide in dichloromethane was added dropwise to a stirred solution of 2.0 mmol of 5-alkyl-1,3-dimethoxybenzene in 20 mL of dichloromethane at 0 °C. The reaction mixture was then stirred at 0 °C for 2 h and allowed to warm to room temperature over a period of time ranging between 6 h to 16 h. Upon completion, the reaction mixture was cooled in an ice bath and cold water was added cautiously. The organic layer was separated and washed with

H₂O, brine, and dried. Filtration, solvent removal, and purification by flash column chromatography (33% acetone–petroleum ether) provided 5-alkylresorcinol in a yield of 85 to 95%.

General Procedure B: Synthesis of (–)-3-Alkyl-Δ⁸-tetrahydrocannabinol (1a–e). A mixture of 1.0 mmol of the 5-alkylresorcinol, 1.1 mmol of (+)-*cis/trans*-*p*-mentha-2,8-dien-1-ol and 0.1 mmol of *p*-toluenesulfonic acid monohydrate in 5–10 mL of anhydrous chloroform was stirred and heated at 65 °C for 6 h. Upon completion, the reaction mixture was cooled and diluted with 10 mL of dichloromethane and stirred with 10 mL of saturated aqueous NaHCO₃ solution for 15 min. The organic layer was then separated and washed with H₂O, brine, and dried over Na₂SO₄. Filtration, concentration and purification by flash column chromatography (10% ethyl acetate–petroleum ether) provided the 3-alkyl-Δ⁸-tetrahydrocannabinol in a yield of 43 to 84%.

4-(1-Adamantanyl)-2,6-dimethoxyphenol (4). A mixture of 5.0 g (32 mmol) of 2,6-dimethoxyphenol and 5.0 g (33 mmol) of 1-adamantanol in 15 mL of 99% methanesulfonic acid was stirred at 80 °C for 3 h and then at room temperature overnight. The reaction mixture was poured onto ice and water and then extracted with dichloromethane. The extract was washed with H₂O, saturated aqueous NaHCO₃, H₂O, brine, and dried over Na₂SO₄. Evaporation of solvent followed by flash column chromatography (30% acetone–petroleum ether) provided 6.0 g of **4** in 64% yield as a white solid, mp 111–112 °C; ¹H NMR δ 6.59 (s, 2H), 5.39 (s, 1H), 3.90 (s, 6H), 2.09 (br s, 3H), 1.89 (d, *J* = 2.2 Hz, 6H), 1.79 (d, *J* = 12.2 Hz, 3H), 1.77 (d, *J* = 12.2 Hz, 3H); MS *m/z* 288 (M⁺).

4-(1-Adamantanyl)-2,6-dimethoxyphenyl Diethyl Phosphate (5). To a solution of 5.5 g (19 mmol) of **4** in 30 mL of freshly distilled CCl₄ was added 3.1 g (22 mmol) of diethyl phosphonate at 0 °C followed by dropwise addition of 3 mL of triethylamine. The mixture was stirred at 0 °C for 1 h and then at room temperature overnight. The mixture was diluted with 70 mL of dichloromethane, washed with H₂O, 4 N NaOH, H₂O, 1 N HCl, H₂O, brine, and dried. Removal of solvent and purification using flash column chromatography (25% acetone–petroleum ether) afforded 7.8 g of **5** in 96.8% yield as a white solid, mp 78–80 °C; ¹H NMR (CDCl₃) δ 6.58 (s, 2H), 4.34–4.22 (m, especially two q, *J* = 8.5 Hz, 4H), 3.86 (s, 3H), 3.85 (s, 3H), 2.09 (br s, 3H), 1.87 (bs, 6H), 1.80 (d, *J* = 13.7 Hz, 3H), 1.76 (d, *J* = 13.7 Hz, 3H), 1.42–1.34 (m, especially two t, *J* = 6.8 Hz, 6H); MS *m/z* 424 (M⁺).

5-(1-Adamantyl)-1,3-dimethoxybenzene (3a). A solution of 7.8 g (18.4 mmol) of **5** in 20 mL of Et₂O and 4 mL of THF was added dropwise to 50 mL of liquid NH₃ at –78 °C as a total 0.3 g of Li metal was added at a rate to maintain a blue color solution. After 1 h, excess Li was treated with NH₄Cl powder, and 100 mL of water-saturated Et₂O was added cautiously. The mixture was brought up to room temperature, and the residual liquid NH₃ was allowed to evaporate. The residual mixture was washed with H₂O, 4 N NaOH, H₂O, brine, and dried. Removal of solvent afforded 3.90 g of a yellow oil which upon chromatographic purification gave 3.62 g of **3a** in 70% yield as a white solid, mp 47–48 °C; ¹H NMR δ 6.55 (d, *J* = 2.3 Hz, 2H), 6.30 (t, *J* = 2.3 Hz, 1H), 3.79 (s, 6H), 2.10 (br s, 3H), 1.90 (d, *J* = 2.6 Hz, 6H), 1.81 (d, *J* = 12.5 Hz, 3H), 1.77 (d, *J* = 12.5 Hz, 3H); MS *m/z* 272 (M⁺).

5-(1-Adamantanyl)resorcinol (2a). 2.7 g of **2a** was prepared from 3.6 g (13.3 mmol) of **3a** following general procedure A in 85% yield as a white solid, mp 186–188 °C; ¹H NMR δ 6.42 (d, *J* = 2.1 Hz, 2H), 6.18 (t, *J* = 2.1 Hz, 1H), 5.40 (s, 2H), 2.07 (bs, 3H), 1.85 (d, *J* = 2.4 Hz, 6H), 1.79 (d, *J* = 12.3 Hz, 3H), 1.74 (d, *J* = 12.3 Hz, 3H); MS *m/z* 244 (M⁺).

3-(1-Adamantanyl)-6,6,9-trimethyl-6a,7,10,10a-tetrahydro-6H-benzo[*c*]chromen-1-ol (1a). 3.0 g of **1a** was prepared from 2.3 g (9.4 mmol) of **2a** following general procedure B in 84% yield as a white solid, mp 205–206 °C; ¹H NMR δ 6.43 (d, *J* = 1.5 Hz, 1H), 6.27 (d, *J* = 1.5 Hz, 1H), 5.42 (d, *J* = 3.65 Hz, 1H), 4.84 (s 1H), 3.20 (dd, *J* = 17.0 Hz, *J* = 4 Hz, 1H), 2.70 (dt, *J* = 11 Hz, *J* = 5.0 Hz, 1H), 2.13 (dd, *J* = 13.0 Hz, *J* = 5.0 Hz, 1H), 2.04 (br s, 3H), 1.86–1.82 (m, 8H), especially

1.84, d, *J* = 2.0 Hz, 6H), 1.80–1.69 (m, 10H), 1.38 (s, 3H), 1.11 (s, 3H); MS *m/z* 378 (M⁺). Anal. (C₂₆H₃₄O₂) C, H.

1-Bromo-3,5-dimethoxybenzene (6). 7.4 g (107 mmol) of sodium nitrate in 15 mL of distilled water was added in small portions to a solution of 10.0 g (65.3 mmol) 3,5-dimethoxyaniline in 30 mL of 48% hydrobromic acid at 0 °C until the stable presence of diazonium salt was observed with starch–potassium iodide test paper. In the meantime, a mixture of 5.2 g (36 mmol) of cuprous bromide in 5.2 mL of 48% hydrobromic acid was heated to boiling in another flask. The prepared diazonium salt solution was added in small portions to the cuprous bromide–hydrobromic acid solution, which was maintained at its boiling point. After the addition, the total reaction mixture was stirred and heated for an additional 30 min, and the resulting crude product was purified by steam distillation. 7.84 g of **6** was collected in 55.8% yield as a white solid, mp 63–64 °C; ¹H NMR δ 6.67 (d, *J* = 2.0 Hz, 2H), 6.39 (t, *J* = 2.0 Hz, 1H), 3.78 (s, 6H); MS *m/z* 216, 218 (M⁺).

5-(2-Hydroxy-2-adamantyl)-1,3-dimethoxybenzene (7). A solution of 690 mg (4.6 mmol) of 2-adamantanone in 10 mL of anhydrous THF was added dropwise to a THF solution of 20 mmol of Grignard reagent prepared from 1.0 g (4.6 mmol) of 1-bromo-3,5-dimethoxybenzene **6** and 110 mg (4.6 mmol) of magnesium chips. The reaction mixture was stirred and heated in a 90 °C oil bath for 2 h and then treated with 20 mL of saturated aqueous NH₄Cl at room temperature with stirring. THF was then removed and the residue was extracted with ether. The ether layer was separated and washed with H₂O, brine, and dried. Filtration, removal of solvent, and purification by flash column chromatography (30% acetone–petroleum ether) afforded 830 mg of **7** in 63.6% yield as a white solid, mp 104–105 °C; ¹H NMR δ 6.70 (d, *J* = 2.2 Hz, 2H), 6.39 (t, *J* = 2.2 Hz, 1H), 3.80 (s, 6H), 2.48 (bs, 2H), 2.39–2.37 (m, 2H), 1.89 (bs, 1H), 1.73–1.70 (m, 8H), 1.53 (bs, 2H); MS *m/z* 288 (M⁺).

5-(2-Adamantyl)-1,3-dimethoxybenzene (3b). A solution of 600 mg (2 mmol) of **7** in 6 mL of anhydrous THF was added dropwise to a flask containing a mixture of 120 mg of lithium and 16 mL of liquid NH₃ at –60 °C. The reaction mixture was stirred vigorously for 2 h at –60 °C. The reaction was warmed to room temperature, and then quenched by the addition of 480 mg of NH₄Cl powder. Then, 25 mL of ether was added to the reaction mixture to extract the product. After the NH₃ had evaporated, the ether solution was separated and washed with H₂O, brine, and dried. Filtration, solvent removal and purification by flash column chromatography (10% acetone–petroleum ether) afforded 420 mg of **3b** in 78% yield as a white solid, mp 72–73 °C; ¹H NMR δ 6.52 (d, *J* = 2.0 Hz, 2H), 6.30 (t, *J* = 2.0 Hz, 1H), 3.79 (s, 6H), 2.93 (s, 1H), 2.41 (bs, 2H), 2.00–1.85 (m, 7H), 1.76 (m, 3H), 1.56 (d, *J* = 8.5 Hz, 2H); MS *m/z* 272 (M⁺).

5-(2-Adamantanyl)resorcinol (2b). 330 mg of **2b** was prepared from 400 mg of **3b** following general procedure A in 92% yield as a white solid, mp 159–160 °C; ¹H NMR (CD₃-COCD₃) δ 7.97 (s, 2H), 6.36 (d, *J* = 2.0 Hz, 2H), 6.18 (t, *J* = 2.0 Hz, 1H), 2.83 (s, 1H), 2.35 (bs, 2H), 2.05–1.87 (m, 7H), 1.77 (bs, 3H), 1.56 (d, *J* = 12.5 Hz, 2H); MS *m/z* 244 (M⁺).

3-(2-Adamantanyl)-6,6,9-trimethyl-6a,7,10,10a-tetrahydro-6H-benzo[*c*]chromen-1-ol (1b). 55 mg of **1b** was prepared from 80 mg of **2b** following general procedure B in 48.5% yield as a white solid, mp 103–105 °C; ¹H NMR δ 6.43 (d, *J* = 2.1 Hz, 1H), 6.25 (d, *J* = 2.1 Hz, 1H), 5.42 (d, *J* = 4.0 Hz, 1H), 4.67 (s, 1H), 3.20 (dd, *J* = 16.5, *J* = 4.0 Hz, 1H), 2.84 (s, 1H), 2.70 (m, 1H), 2.34 (br d, *J* = 6 Hz, 2H), 2.15 (m, 1H), 1.96–1.74 (m, 13H), 1.70 (s, 3H), 1.52 (m, 2H), 1.38 (s, 3H), 1.15 (s, 3H); MS *m/z* 378 (M⁺). Anal. (C₂₆H₃₄O₂) C, H.

5-(2-Hydroxy-2-adamantyl)methyl-1,3-dimethoxybenzene (8). A solution of 2.72 g (18 mmol) 2-adamantanone in 15 mL of anhydrous ether was added dropwise to an ether solution of 20 mmol of Grignard reagent prepared from 3.72 g (20 mmol) of 3,5-dimethoxybenzyl chloride and 0.5 g (20.8 mmol) of magnesium chips. The reaction mixture was stirred for 1 h, and then quenched with 15 mL of saturated aqueous NH₄Cl. The ether layer was separated and washed with H₂O,

brine, and dried. Filtration, removal of solvent and purification by flash column chromatography (30% acetone–petroleum ether) afforded 4.30 g of **8** in 79.7% yield as a white solid, mp 75–77 °C; $^1\text{H NMR}$ δ 6.40 (d, $J = 2.2$ Hz, 2H), 6.37 (t, $J = 2.2$ Hz, 1H), 3.78 (s, 6H), 2.94 (s, 2H), 2.17–2.03 (m, 4H), 1.92 (bs, 1H), 1.81–1.70 (m, 6H), 1.59–1.52 (m, 4H); MS *m/z* 284 ($\text{M}^+ - \text{H}_2\text{O}$).

5-(2-Adamantylidene)methyl-1,3-dimethoxybenzene (3c). A mixture of 2.0 g of **8** and 0.2 g of *p*-toluenesulfonic acid monohydrate in 20 mL of dichloromethane was stirred and heated at 45 °C overnight. The reaction mixture was then treated with 10% aqueous NaHCO_3 solution. The organic layer was separated and washed with H_2O , brine, and dried. Filtration, concentration and purification by flash column chromatography (15% acetone–petroleum ether) afforded 1.70 g of **3c** in 83% yield as a white solid, mp 51–52 °C; $^1\text{H NMR}$ δ 6.37 (d, $J = 1.8$ Hz, 2H), 6.32 (t, $J = 1.8$ Hz, 1H), 6.12 (s, 1H), 3.78 (s, 6H), 3.18 (bs, 1H), 2.47 (br s, 1H), 1.99–1.85 (m, 12H); MS *m/z* 284 (M^+).

5-(2-Adamantylidene)methylresorcinol (2c). 320 mg of **2c** was prepared from 400 mg of **3c** following general procedure A in 88% yield as a white solid, mp 144–146 °C; $^1\text{H NMR}$ ($\text{CD}_3\text{-COCD}_3$) δ 8.07 (bs, 2H), 6.21 (d, $J = 1.8$ Hz, 2H), 6.20 (t, $J = 1.8$ Hz, 1H), 6.06 (s, 1H), 3.20 (bs, 1H), 2.44 (bs, 1H), 1.97–1.79 (m, 12H); MS *m/z* 256 (M^+).

3-(2-Adamantylidene)methyl-6,6,9-trimethyl-6a,7,10,10a-tetrahydro-6H-benzo[*c*]chromen-1-ol (1c). 120 mg of **1c** was prepared from 144 mg of **2c** following general procedure B in 40% yield as a white solid, mp 98–100 °C; $^1\text{H NMR}$ δ 6.30 (d, $J = 1.3$ Hz, 1H), 6.12 (d, $J = 1.3$ Hz, 1H), 5.99 (s, 1H), 5.43 (br d, $J = 4.5$ Hz, 1H), 4.70 (s, 1H), 3.23 (bs, 1H), 3.18 (dd, $J = 16.5$, $J = 4.5$ Hz, 1H), 2.71 (td, 1H), 2.43 (bs, 1H), 2.14 (m, 1H), 1.98–1.79 (m, 15H), 1.76 (s, 3H), 1.37 (s, 3H), 1.10 (s, 3H); MS *m/z* 390 (M^+). Anal. ($\text{C}_{27}\text{H}_{34}\text{O}_2 \cdot \text{H}_2\text{O}$) C, H.

5-(2-Adamantyl)methyl-1,3-dimethoxybenzene (3d). A mixture of 800 mg **3c** and 100 mg of 10% Pd–C in 25 mL of anhydrous ethanol was hydrogenated on Parr hydrogenation shaker at 45 psi. Upon completion of hydrogenation, filtration of palladium catalyst, and solvent removal, 785 mg of **3d** was collected in a yield of 98% as a low melting point solid, mp 31–32 °C; $^1\text{H NMR}$ δ 6.34 (d, $J = 2.2$ Hz, 2H), 6.29 (t, $J = 2.2$ Hz, 1H), 3.77 (s, 6H), 2.67 (d, $J = 7.5$ Hz, 2H), 1.99 (d, $J = 12.0$ Hz, 2H), 1.93 (t, $J = 8.0$ Hz, 1H), 1.85–1.79 (m, 4H), 1.72–1.67 (m, 6H), 1.56 (d, $J = 12.0$ Hz, 2H); MS *m/z* 286 (M^+).

5-(2-Adamantyl)methylresorcinol (2d). 370 mg of **2d** was prepared from 520 mg of **3d** following general procedure A in 79% yield as white solid, mp 147–149 °C; $^1\text{H NMR}$ δ 6.12 (d, $J = 1.5$ Hz, 2H), 6.07 (t, $J = 1.5$ Hz, 1H), 2.59 (d, $J = 8.0$ Hz, 2H), 2.06 (d, $J = 12.5$ Hz, 2H), 1.91 (t, $J = 7.8$ Hz, 1H), 1.86–1.84 (m, 4H), 1.76–1.71 (m, 4H), 1.65 (bs, 2H), 1.57 (d, $J = 12.5$ Hz, 2H); MS *m/z* 258 (M^+).

3-(2-Adamantyl)methyl-6,6,9-trimethyl-6a,7,10,10a-tetrahydro-6H-benzo[*c*]chromen-1-ol (1d). 300 mg of **1d** was prepared from 341 mg of **2d** following general procedure B in 57% yield as a white solid, mp 94–96 °C; $^1\text{H NMR}$ δ 6.25 (d, $J = 2.4$ Hz, 1H), 6.09 (d, $J = 2.4$ Hz, 1H), 5.42 (d, $J = 4.3$ Hz, 1H), 4.65 (s, 1H), 3.19 (dd, $J = 16.5$, $J = 4.0$ Hz, 1H), 2.68 (td, $J = 10.6$, $J = 4.6$ Hz, 1H), 2.56 (m, 2H), 2.13 (m, 1H), 1.98 (d, $J = 12.5$ Hz, 1H), 1.95 (t, $J = 7.5$ Hz, 1H), 1.91–1.78 (m, 8H), 1.71–1.67 (m, 9H, especially 1.69, s, CH_3), 1.53 (br d, $J = 12.5$ Hz, 2H), 1.37 (s, 3H), 1.10 (s, 3H); MS *m/z* 392 (M^+). Anal. ($\text{C}_{27}\text{H}_{36}\text{O}_2$) C, H.

5-(1-Adamantyl)methyl-1,3-dimethoxybenzene (3e). A solution of 645 mg (3 mmol) of 1-bromoadamantane in 15 mL of anhydrous ether was added dropwise to a 20 mL ether solution of Grignard reagent prepared from 560 mg (3 mmol) of 3,5-dimethoxybenzyl chloride and 77 mg (3.2 mmol) of magnesium chips. The reaction mixture was stirred and refluxed for 3 h. Then, the ether was gradually removed with an argon gas stream, and the highly concentrated residue was heated at 90 °C for 8 h. The reaction mixture was then treated with 15 mL of saturated aqueous NH_4Cl solution at room temperature and extracted with ether. The ether layer was separated, washed with H_2O , brine, and dried. Filtration,

solvent removal and purification by flash column chromatography (10% acetone–petroleum ether) afforded 210 mg of **3e** in 24% yield as colorless oil; $^1\text{H NMR}$ δ 6.33 (t, $J = 2.1$ Hz, 1H), 6.25 (d, $J = 2.1$ Hz, 2H), 3.78 (s, 6H), 2.31 (s, 2H), 1.93 (bs, 3H), 1.67–1.64 (m, 2H), 1.58–1.55 (m, 4H), 1.49 (bs, 6H); MS *m/z* 286 (M^+).

5-(1-Adamantyl)methylresorcinol (2e). 150 mg of **2e** was prepared from 190 mg of **3e** following general procedure A in 89.3% yield as a white solid, mp 163–164 °C; $^1\text{H NMR}$ δ 6.20 (t, $J = 1.6$ Hz, 1H), 6.15 (d, $J = 1.6$ Hz, 2H), 4.72 (bs, 2H), 2.25 (bs, 2H), 1.92 (bs, 3H), 1.67–1.55 (m, 6H), 1.47 (bs, 6H); MS *m/z* 258 (M^+).

3-(1-Adamantyl)methyl-6,6,9-trimethyl-6a,7,10,10a-tetrahydro-6H-benzo[*c*]chromen-1-ol (1e). 85 mg of **1e** was prepared from 130 mg of **2e** following the general procedure B in 43.4% yield as a white solid, mp 84–85 °C; $^1\text{H NMR}$ δ 6.17 (d, $J = 1.5$ Hz, 1H), 6.01 (d, $J = 1.5$ Hz, 1H), 5.42 (d, $J = 4.2$ Hz, 1H), 4.64 (bs, 1H), 3.20 (dd, $J = 17.0$ Hz, $J = 3.5$ Hz, 1H), 2.70 (dt, $J = 10.5$, $J = 4.5$ Hz, 1H), 2.23 (d, $J = 12.5$ Hz, 1H), 2.18 (d, $J = 12.5$ Hz, 1H), 2.17–2.12 (m, 1H), 1.92 (bs, 3H), 1.82 (m, 2H), 1.70 (s, 3H), 1.64 (br d, $J = 12.5$ Hz, 3H), 1.58 (br d, $J = 12.5$ Hz, 3H), 1.50 (m, 1H), 1.47 (bs, 6H), 1.37 (s, 3H), 1.10 (s, 3H); MS *m/z* 392 (M^+). Anal. ($\text{C}_{27}\text{H}_{36}\text{O}_2 \cdot 1/2\text{H}_2\text{O}$) C, H.

Radioligand Binding Assay. Forebrain synaptosomal membranes were prepared from frozen rat brains by the method of Dodd et al.²⁷ and were used to assess the affinities of the novel analogues for the CB1 binding sites, while affinities for the CB2 sites were measured using a membrane preparation from frozen mouse spleen using a similar procedure.²⁸ The displacement of specifically tritiated CP-55,940 from these membranes was used to determine the IC_{50} values for the test compounds. The assay was conducted in a 96-well microfilter plate. The samples were filtered using a Packard Filtermate Harvester and Whatman GF/B unfilter-96 plates, and 0.5% BSA was incorporated into the wash buffer. Radioactivity was detected using MicroScint 20 scintillation cocktail added to the dried filter plates and was counted using a Packard Instruments Top Count. Data were collected from three independent experiments between 100% and 0% specific binding for [^3H]CP-55,940, determined using 0 and 100 nM CP-55,940. The normalized data from three independent experiments were combined and analyzed using a four-parameter logistic equation to yield IC_{50} values which were converted to K_i values using the assumptions of Cheng and Prusoff.²⁹

Computational Study. Conformational Analyses. The structures of **1a–e** were built in the Spartan molecular modeling program (V4.1.1; Wavefunction, Inc., Irvine, CA) initially in the global minimum energy conformation of (–)- Δ^8 -THC.³⁷ Each structure was then energy minimized using the AM1 semiempirical method as encoded in Spartan. AM1 conformational searches were performed for each side chain rotatable bond. This search included a 12-fold rotation about the C3–C1' bond for **1a**, the C3–C2' bond for **1b**, and the C3–C1'' bond for **1c**. For **1d** and **1e**, 12-fold rotations were performed about the C3–C1'' bond and about the C1''–C2' bond in **1d** and the C1''–C1' bond in **1e**. The results of these conformational searches were used to identify the global minimum energy conformer of each compound and to determine the energy separation between the global minimum energy conformer and other minimum energy conformers identified by the AM1 conformational analysis. For each compound, conformers were considered accessible at biological temperature if their energies were less than 2.0 kcal/mol above the global minimum energy. Conformational analysis results are graphically represented in Figures 2 and 3.

Unique Volume Map Calculation. To illustrate the key conformational differences between the CB1 selective 3-(1-adamantyl)-THC **1a** and the CB2 selective 3-(2-adamantyl)-methyl-THC **1c**, we used a modification of the Active Analog Approach³⁰ to calculate the volume of space that is unique to the CB2 selective analogue **1c**. All accessible conformers identified for **1a** and **1c** were superimposed at their aromatic

rings. Using the DEF MAP, SET MAP, and COMBINE MAP facilities within the Chem-X molecular modeling suite of programs (v2000.1; Oxford Molecular, Inc.) and a density of 4 points per Å, the van der Waals (VdW's) volume map of each of the conformers identified for **1a** and for **1c** was calculated. The UNION of the VdW's volume maps of the CB1-selective compound **1a** was calculated and is illustrated as a purple grid in Figure 4a. Similarly, the UNION of the VdW's volume maps of the CB2-selective compound **1c** was calculated. Using a logical NOT operation, the region of space that the conformers of **1c** did not share with that of **1a** was then calculated. This Unique Volume Map is illustrated as a yellow grid in Figure 4b. A similar protocol was followed to calculate the volume unique to the CB2 selective compound **1c** relative to the nonselective compound **1d** (red grid, Figure 4c).

Crystallography of 3-(1-Adamantanyl)-6,6,9-trimethyl-6a,7,10,10a-tetrahydro-6H-benzo[c]chromen-1-ol (1a). The molecular formula of **1a** is C₂₆H₃₄O₂, and the formula weight is 378.55. An irregular colorless crystal of **1a** with dimensions 0.11 × 0.34 × 0.42 mm² was grown from a two-phase solvent system (hexane (top) and dichloromethane (bottom)). Crystallographic data were collected on a Bruker three-circle platform diffractometer equipped with a SMART 1000 CCD detector. The crystals were irradiated using graphite monochromated Mo K α radiation ($\lambda = 0.71073$). An MSC X-Stream low-temperature device was used to keep the crystals at a constant -180 °C during data collection. Data collection was performed and the unit cell was initially refined using SMART v5.625 (Bruker 2001a, SMART v5.625. Bruker AXS Inc., Madison, WI). Data reduction was performed using SAINT v6.26A (Bruker, 2002, SAINT v6.26A. Bruker AXS Inc., Madison, WI) and XPREP v6.12 (Bruker, 2001b, XPREP v6.12. Bruker AXS Inc., Madison, WI). Corrections were applied for Lorentz, polarization, and absorption effects using SADABS v2.03 (Bruker, 2000, SADABS v2.03, Bruker AXS Inc., Madison, WI). The structure was solved and refined with the aid of the programs in the SHELXTL-plus v6.12 system of programs (Bruker, 2000, SHELXTL v6.12. Bruker AXS Inc., Madison, WI). The full-matrix least-squares refinement on F^2 included atomic coordinates and anisotropic thermal parameters for all non-H atoms. The H atoms were included using a riding model. The crystal of **1a** was orthorhombic and space group $P2_12_12_1$ with cell dimensions: $a = 11.863(5)$ Å, $b = 13.186(6)$ Å, $c = 13.788(6)$ Å, and volume of 2157.0(17) Å³, $Z = 4$. Calculated density was 1.166 mg/mm³. Absorption coefficient was 0.071 mm⁻¹. Final R indices were 0.0437 for 4321 observed ($I > 2\sigma I$) reflections and 0.0547 for all 4996 reflections. Goodness-of-fit equals to 1.017, 256 parameters. Complete data for bond lengths and angles are available in the Supporting Information.

Methods for in Vivo Study of Compound 1a. Apparatus. Drug discrimination training and testing were conducted in 8 operant chambers (ENV-001, Med. Associates, St Albans/Georgia, VT), constructed of Plexiglas and aluminum, equipped with two response levers, house and lever lights, and a grid floor. Each chamber was enclosed within sound- and light-attenuating boxes equipped with an exhaust fan. These chambers were connected to an IBM-compatible PC.

Animals. Adult male Sprague-Dawley rats ($n = 8$; Taconic Farms, Germantown, NY) were individually housed in a colony room with an average temperature of 20 °C and a 12-h light/dark cycle (rats were trained and tested during the light phase). Purina Rat Chow was restricted to approximately 12 g/day, thus maintaining body weights between 330 and 400 g.

Training. Rats were magazine trained, and shaped to lever press for food reinforcement until they responded 10 times for each reinforcer (FR 10). Each reinforcement consisted of two 45 mg Noyes pellets. The rats were then trained in a two-choice task to respond on drug- or vehicle-appropriate levers once daily. The position of drug-appropriate levers was randomly assigned among subjects so that it was to the right of the food cup for half the subjects. Animals were administered 3 mg/kg Δ^9 -THC or vehicle (2 mL/kg) intraperitoneally 30 min before session onset. Presses on the wrong lever were recorded, but had no programmed consequences. The schedule of drug (D)

or vehicle (N) administrations was nonsystematic, with no more than two consecutive D or N trials. There was approximately an equal number of D and N training sessions throughout the study. To avoid the influence of odor cues left in a chamber by a preceding subject,³⁸ the order in which D and N training sessions were conducted for animals trained in the same chamber was randomized. Training sessions were conducted Monday through Friday and lasted 20 min. Training continued until animals reached the acquisition criterion of selecting the injection-appropriate (D or N) lever on at least 8 out of 10 consecutive training days. Correct selection was defined as total presses before the first reinforcement being equal or less than 14 (i.e., an animal did not press the wrong lever more than 4 times before pressing 10 times on the appropriate lever).

Testing. After animals reached acquisition criterion, test sessions were conducted on average 3 times every two weeks; on interim days, training sessions were conducted. A drug training session preceded half the test sessions; the other half was preceded by a vehicle session. Tests were conducted only if responding during the preceding training sessions had been correct. During testing, animals were reinforced for 10 presses on either lever until 20 min had elapsed or 6 reinforcers had been delivered, whichever occurred first. A repeated tests procedure^{34,35} was used to assess the time course of **1a**. Thus, rats were injected with a specified dose of **1a** and first put into the experimental chamber 30 min postadministration with above-described reinforcement contingencies in effect. The second test took place 90 min post, and the third (final) test occurred 270 min after administration. Between these trials animals waited in their respective home cages. Doses were examined in a mixed order. Each dose of Δ^9 -THC was examined once (30 min post). For each dose tested, the percentage of responding on the drug-appropriate lever was calculated from the ratio of the number of presses on the Δ^9 -THC-associated lever to the total number of lever presses in a test session. Additionally, response rate (responses per second) was calculated and analyzed with two-way repeated analysis of variance (ANOVA; Sigma Stat., V, 3; SPSS, Chicago, IL). Nonlinear regression analysis of dose-generalization data was performed using Prism 3 software (GraphPad Software, San Diego, CA) to provide ED₅₀ ($\pm 95\%$ confidence limits, 95% C.L.).

Drugs. (-)- Δ^9 -THC, dissolved in ethanol (200 mg/mL), was kindly provided by NIDA (batch 7074-91) and stored at -20 °C until used. Upon arrival, **1a** was also dissolved in ethanol, appropriate amounts were withdrawn, the ethanol was evaporated under a stream of nitrogen, and the residue was then dissolved in a solution of 5% propylene glycol and 3% Tween-80 and stored at -20 °C. Shortly before being used, the solute was diluted with normal (0.9%) saline after the solute had been sonicated for 20-30 min. This procedure was followed for preparing suspensions of Δ^9 -THC as well. SR141716A (Sanofi Recherche, France) was stored at room temperature in crystalline form and dissolved in the propylene glycol/Tween-80 (5%/3%) mixture before being diluted with saline (92%). Drugs were administered ip 2 mL/kg.

Acknowledgment. This work was supported by grants from the National Institute on Drug Abuse DA03801, DA09158, and DA07215 (Northeastern University), and DA09064 and DA00253 (Temple University). We are grateful to Richard Duclos for assistance with the manuscript.

Supporting Information Available: Crystal structure data for analogue **1a**, detailed conformational analysis results for compounds **1a-e**, and elemental analysis results for compounds **1a-e**. This material is available free of charge via the Internet at <http://pubs.acs.org>.

References

- (1) Gaoni, Y.; Mechoulam, R. Isolation, structure, and partial synthesis of an active constituent of hashish. *J. Am. Chem. Soc.* **1964**, *86*, 1646-1647.

- (2) Devane, W. A.; Dysarz, F. A., III.; Johnson, M. R.; Melvin, L. S.; Howlett, A. C. Determination and characterization of a cannabinoid receptor in rat brain. *Mol. Pharmacol.* **1988**, *34*, 605–613.
- (3) Matsuda, L. A.; Lolait, S. J.; Brownstein, M. J.; Young, A. C.; Bonner, T. I. Structure of a cannabinoid receptor and functional expression of the cloned cDNA. *Nature* **1990**, *346*, 561–564.
- (4) Munro, S.; Thomas, K. L.; Abu-Shaar, M. Molecular characterization of a peripheral receptor for cannabinoids. *Nature* **1993**, *365*, 61–65.
- (5) Pertwee, R. G. Pharmacology of cannabinoid CB1 and CB2 receptors. *Pharmacol. Ther.* **1997**, *74*, 129–180.
- (6) Razdan, R. K. Structure–activity relationships in cannabinoids. *Pharmacol. Rev.* **1986**, *38*, 75–149.
- (7) Pertwee, R. G. Pharmacology of cannabinoid receptor ligands. *Curr. Med. Chem.* **1999**, *6*, 635–664.
- (8) Palmer, S. L.; Thakur, G. A.; Makriyannis, A. Cannabinergic ligands. *Chem. Phys. Lipids* **2002**, *121*, 3–19.
- (9) Khanolkar, A. D.; Palmer, S. L.; Makriyannis, A. Molecular probes for the cannabinoid receptors. *Chem. Phys. Lipids* **2000**, *108*, 37–52.
- (10) Makriyannis, A.; Rapaka, R. S. The molecular basis of cannabinoid activity. *Life Sci.* **1990**, *47*, 2173–2184.
- (11) Adams, R. Marijuana. *Harvey Lectures* **1942**, *37*, 168–197.
- (12) Adams, R.; Harfenist, M.; Lowe, S. New analogues of tetrahydrocannabinol. XIX. *J. Am. Chem. Soc.* **1949**, *71*, 1624–1628.
- (13) Huffman, J. W.; Miller, J. R. A.; Liddle, J.; Yu, S.; Thomas, B. F.; Wiley, J. L.; Martin, B. R. Structure–activity relationships for 1',1'-dimethylalkyl- Δ^8 -tetrahydrocannabinols. *Bioorg. Med. Chem.* **2003**, *11*, 1397–1410.
- (14) Huffman, J. W.; Liddle, J.; Duncan, S. G., Jr.; Yu, S.; Martin, B. R.; Wiley, J. L. Synthesis and pharmacology of the isomeric methylheptyl- Δ^8 -tetrahydrocannabinols. *Bioorg. Med. Chem.* **1998**, *6*, 2383–2396.
- (15) Papahatjis, D. P.; Kourouli, T.; Abadji, V.; Goutopoulos, A.; Makriyannis, A. Pharmacophoric requirements for cannabinoid side chains: multiple bond and C1'-substituted Δ^8 -tetrahydrocannabinols. *J. Med. Chem.* **1998**, *41*, 1195–1200.
- (16) Busch-Petersen, J.; Hill, W. A.; Fan, P.; Khanolkar, A.; Xie, X.-Q.; Tius, M. A.; Makriyannis, A. Unsaturated side chain β -11-hydroxyhexahydrocannabinol analogues. *J. Med. Chem.* **1996**, *39*, 3790–3796.
- (17) Papahatjis, D. P.; Nikas, S. P.; Andreou, T.; Makriyannis, A. Novel 1',1'-chain substituted Δ^8 -tetrahydrocannabinols. *Bioorg. Med. Chem. Lett.* **2002**, *12*, 3583–3586.
- (18) Papahatjis, D. P.; Nikas, S. P.; Kourouli, T.; Chari, R.; Xu, W.; Pertwee, R. G.; Makriyannis, A. Pharmacophoric requirements for the cannabinoid side chain. Probing the cannabinoid receptor subsite at C1'. *J. Med. Chem.* **2003**, *46*, 3221–3229.
- (19) Khanolkar, A. D.; Lu, D.; Fan, P.; Tian, X.; Makriyannis, A. Novel conformationally restricted tetracyclic analogs of Δ^8 -tetrahydrocannabinol. *Bioorg. Med. Chem. Lett.* **1999**, *9*, 2119–2124.
- (20) Luk, T.; Jin, W.; Zvonok, A.; Lu, D.; Lin, X.-Z.; Chavkin, C.; Makriyannis, A.; Mackie, K. Identification of a potent and highly efficacious, yet slowly desensitizing CB1 cannabinoid receptor agonist. *Br. J. Pharmacol.* **2004**, *142*, 495–500.
- (21) Järbe, T. U. C.; DiPatrizio, N. V.; Lu, D.; Makriyannis, A. (–)-Adamantyl- Δ^8 -tetrahydrocannabinol (AM411), a selective cannabinoid CB₁ receptor agonist: effects on open-field behaviors and antagonism by SR-141716 in rats. *Behav. Pharmacol.* **2004**, *15*, 517–521.
- (22) Petrzilka, T.; Haeflinger, W.; Sikemeier, C. Synthese von Haschisch-Inhaltsstoffen. *Helv. Chim. Acta* **1969**, *52*, 1102–1134.
- (23) Franke, I.; Binder, M. Synthesis of cannabinoid model compounds. Part 2. (3R,4R)- $\Delta^{1(6)}$ -Tetrahydrocannabinol-5'-oic acid and 4''(R,S)-methyl-(3R,4R)- $\Delta^{1(6)}$ -tetrahydrocannabinol-5'-oic acid. *Helv. Chim. Acta* **1980**, *63*, 2508–2514.
- (24) Dominianni, S. J.; Ryan, C. W.; DeArmitt, C. W. Synthesis of 5-(tert-alkyl)resorcinols. *J. Org. Chem.* **1977**, *42*, 344–346.
- (25) Ohno, M.; Shimizu, K.; Ishizaki, K.; Sasaki, T.; Eguchi, S. Cross-coupling reaction of tert-alkyl halides with Grignard reagents in dichloromethane as a non-Lewis basic medium. *J. Org. Chem.* **1988**, *53*, 729–733.
- (26) Osawa, E.; Majerski, Z.; Schleyer, P. V. R. Preparation of bridgehead alkyl derivatives by Grignard coupling. *J. Org. Chem.* **1971**, *36*, 205–207.
- (27) Dodd, P. R.; Hardy, J. A.; Oakley, A. E.; Edwardson, J. A.; Perry, E. K.; Delaunoy, J. P. A. rapid method for preparing synaptosomes: comparison, with alternative procedures. *Brain Res.* **1981**, *226*, 107–118.
- (28) Khanolkar, A. D.; Abadji, V.; Lin, S.; Hill, W. A. G.; Taha, G.; Abouzid, K.; Meng, Z.; Fan, P.; Makriyannis, A. Head group analogues of arachidonylethanolamide, the endogenous cannabinoid ligand. *J. Med. Chem.* **1996**, *39*, 4515–4519.
- (29) Cheng, Y. C.; Prusoff, W. H. Relationship between the inhibition constant (K_i) and the concentration of inhibitor which causes 50% inhibition (IC₅₀) of an enzymatic reaction. *Biochem. Pharmacol.* **1973**, *22*, 3099–3102.
- (30) Sufirin, J. R.; Dunn, D. A.; Marshall, G. R. Steric mapping of the L-methionine binding site of ATP: L-methionine S-adenosyltransferase. *Mol. Pharmacol.* **1981**, *19*, 307–313.
- (31) Ottersen, T.; Rosenqvist, E.; Turner, C. E.; El-Feraly, F. S. The crystal and molecular structure of cannabidiol. *Acta Chem. Scand. B* **1977**, *31*, 807–812.
- (32) Rosenqvist, E.; Ottersen, T. The crystal and molecular structure of Δ^9 -tetrahydrocannabinolic acid b. *Acta Chem. Scand. B* **1975**, *29*, 379–384.
- (33) Järbe, T. U. C.; Hiltunen, A. J.; Mechoulam, R. Stereospecificity of the discriminative stimulus functions of the dimethylheptyl homologs of 11-hydroxy- Δ^8 -tetrahydrocannabinol in rats and pigeons. *J. Pharm. Exp. Ther.* **1989**, *250*, 1000–1005.
- (34) Järbe, T. U. C.; Swedberg, M. D. B.; Mechoulam, R. A repeated tests procedure to assess onset and duration of the cue properties of (–)- Δ^9 -THC, (–)- Δ^8 -THC-DMH and (+)- Δ^8 -THC. *Psychopharmacology* **1981**, *75*, 152–157.
- (35) Järbe, T. U. C.; Hiltunen, A. J.; Lander, N.; Mechoulam, R. Cannabimimetic activity (Δ^1 -THC cue) of cannabidiol monomethyl ether and two stereoisomeric hexahydrocannabinols in rats and pigeons. *Pharmacol. Biochem. Behav.* **1986**, *25*, 393–399.
- (36) Rinaldi-Carmona, M.; Barth, F.; Héaulme, M.; Shire, D.; Calandra, B.; Congy, C.; Martinez, S.; Maruani, J.; Néliat, G.; Caput, D. et al. SR141716A, a potent and selective antagonist of the brain cannabinoid receptor. *FEBS. Lett.* **1994**, *350*, 240–244.
- (37) Reggio, P. H.; Panu, A. M.; Miles S. Characterization of a region of steric interference at the cannabinoid receptor using the active analogue approach. *J. Med. Chem.* **1993**, *36*, 1761–1771.
- (38) Extance, K.; Goudie, A. J. Inter-animal olfactory cues in operant drug discrimination procedures in rats. *Psychopharmacology* **1981**, *73*, 363–371.

JM058175C